

Article

# Feedback Linearization Based Robust Control for Linear Permanent Magnet Synchronous Motors

Yung-Te Chen <sup>1</sup>, Chi-Shan Yu <sup>2</sup> and Ping-Nan Chen <sup>3,\*</sup>

<sup>1</sup> Graduate Institute of Applied Science and Technology, National Taiwan University of Science and Technology, Taipei 106, Taiwan; alum438217@gmail.com

<sup>2</sup> Department of Digital Technology Design, National Taipei University of Education, Taipei 106, Taiwan; chsyu@tea.ntue.edu.tw

<sup>3</sup> Department of Biomedical Engineering, National Defense Medical Center, Taipei 114, Taiwan

\* Correspondence: g931310@gmail.com; Tel.: +886-2-87923100

Received: 25 August 2020; Accepted: 6 October 2020; Published: 9 October 2020



**Abstract:** In this study, we designed a feedback linearization control strategy for linear permanent magnet synchronous motors (LPMSMs) as well as a robust control mechanism. First, the highly nonlinear system was transformed into an exact linear system by the feedback linearization technique. Then, we designed a robust controller to mitigate the impact of system parameter disturbances on system performance. This novel robust feedback controller can be applied to electromagnetic force, speed and position control loops in linear motors, correct the errors created by uncertainty factors in the entire system in real time, and set the system's settling time based on the application environment of the plant. Finally, we performed simulations and experiments using a PC-based motor control system, which demonstrated that the proposed robust feedback controller can achieve good performance in the controlled system with robust anti-disturbance control.

**Keywords:** linear permanent magnet synchronous motor; feedback linearization; robust control

## 1. Introduction

Recent advances in electronics and microprocessor technology have enabled the realization of high-performance motor control. Linear permanent magnet synchronous motors (LPMSMs) are capable of greater torque (both steady-state and transient) than linear induction motors (LIMs) of the same size, while providing superior efficiency. This has led to their widespread application in situations where very fast torque-response and high-performance control are required [1]. Space vector modulation (SVM) control theory is increasingly being applied to LPMSMs [2]. Proportional Integral (PI) controllers are generally used to control the speed and two-axis current control loops of permanent magnet synchronous motors with vector control due to its simplicity and effectiveness. PI controller parameters can be adjusted using the root locus method and pole placement method. However, changes in the parameters and in the load of the controlled system may vary; a conventional PI controller may not perform well over a wide range of operating conditions. Researchers have developed a few methods to produce stable closed-loop systems. In 2015, Huikuri used feedforward compensation to reduce the influence of thrust friction and thrust ripples in linear motors with the aim of improving system tracking performance [3]. In 2009, Ghafari-Kashani applied H-infinity robustness control theory in designing the  $K$  value of the transition matrix in a closed loop system to ensure stability in compliance with existing standards [4]. In 2012, 2013 and 2018, Choi, Ananthamoorthy and Pei used fuzzy control logic to tune the PI controllers of LPMSMs online [5–7].

In recent years, feedback linearization has been an active research area [8,9], and its related results for motor control have become the focus of attention [10–15]. Feedback linearization requires

extremely precise measurements of system parameters to eliminate the effect of nonlinearity from the system and thereby achieve the anticipated effects [11,12,16]. In 2010, Vittek applied feedback linearization to LPMSM; however, he does not consider the issue of parameter fluctuations [17]. In 2015 and 2018, Tang and Lin used robust and adaptive optimal control that can suppress parameter disturbances [12,18]. In 2011 and 2018, Ibtissem, Asseu and Song used sliding model controllers to mediate uncertainties in LIM system parameters [19–21]. In 2010, Wang used Grey system theory to perform relational analysis in uncertain systems with incomplete data and modeling for feedback linearization [22]. The slip model observer and Grey theory was shown to stabilize nonlinear states; however, the methods used in [18–22] are too complicated for most industrial applications.

The main purposes of this thesis are to investigate the feedback linearization control application strategies of linear permanent magnet synchronous motor (LPMSM) and to develop a robust controller to improve the drawbacks of the traditional feedback linearization control scheme due to parameter uncertainties. Then, the highly nonlinear system is transformed to an exact linear system by the feedback linearization technique. Additionally, a robust controller is designed to reduce the control performance degradation due to system parameter variation. Moreover, the newly designed robust feedback linearization control system is implemented for a LPMSM drive to track electromagnetic force, speed and position commands. Finally, MATLAB/SIMULINK software and PC-based hardware are used to verify the feasibilities of this scheme. The experimentation results prove the excellent characteristics of the proposed system. A simple and robust controller design that does not require complex calculations is needed for feedback linearization when the ultimate objective is to enhance the precision of the motor speed and position in a wide range of industrial applications.

The rest of this paper is organized as follows. Section 2 is the dynamic model of linear permanent synchronous motors. Section 3 describes the planning and design of feedback linearization and robust control mechanisms, mainly describing the theory, framework and the design of the robustness control mechanism of feedback linearization. The simulation and testing of software and hardware modules and control software designed in Section 4 and uses vector control as the basis to realize a LPMSM thrust, speed and position control system with feedback linearization and robust control mechanisms. Section 5 presents the results and discussion. Finally, Section 6 presents conclusions for this work.

## 2. Dynamic Model of Linear Permanent Synchronous Motors

In this chapter, we describe the coordinate transformation of the three-phase AC expression of the LPMSM circuit formula into a two-axis DC expression and the application of this formula to vector control. The resulting coordinate transformation method can be used to rewrite the three-phase circuit dynamic equation of LPMSMs as a two-axis dynamic mathematical model in order to elucidate the control characteristics and lay down a foundation for the control method.

The complexity of the three-phase coordinate mathematical expression of LPMSMs makes them unsuitable for motor control. To simplify the mathematical model of the motor, we established a system within a vector control framework based on principles of coordinate transformation. By changing the three-phase variable to a two-phase variable using a power-invariant transformation, the three-phase coordinate system is presented as an easily controllable two-phase d-q axis coordinate system, and the excitation of the stator-side permanent magnet of the LPMSM falls on the d-axis. If the stator current is zero, then the mover current of the motor falls on the q axis, which means that it can be used to control the electromagnetic force of the LPMSM in a simplified motor control system. Assuming a uniform air gap on the surface of the secondary stator excited by the permanent magnet of the motor, then  $L_d = L_q = L_s$  and the dynamic equation of the synchronous rotating coordinate system of the LPMSM is as follows:

$$\begin{bmatrix} \frac{d}{dt} i_d \\ \frac{d}{dt} i_q \end{bmatrix} = \begin{bmatrix} -\frac{R_s}{L_s} & \frac{\pi}{\tau} \dot{\chi}_p \\ -\frac{\pi}{\tau} \dot{\chi}_p & -\frac{R_s}{L_s} \end{bmatrix} \begin{bmatrix} i_d \\ i_q \end{bmatrix} + \frac{1}{L_s} \begin{bmatrix} v_d \\ v_q - \sqrt{\frac{2}{3}} \frac{\pi}{\tau} \varphi_m \dot{\chi}_p \end{bmatrix} \quad (1)$$

The mechanical equation of the LPMSM under the  $d-q$  axis synchronous rotating coordinate system is

$$F = \frac{dW_{abcs}}{dx} = M \frac{d^2x}{dt^2} + B \frac{dx}{dt} + F_L \quad (2)$$

where  $M$  denotes the mass of the mover,  $B$  is the viscous friction coefficient and  $F_L$  is the load of the motor. The total energy of the motor is derived as follows:

$$W_{abcs} = \frac{1}{2} [I_{abcs}^T (L_s - L_{ls} I) I_{abcs} + I_{abcs}^T \varphi_m] \quad (3)$$

where  $I$  is the operation unit matrix. The electromagnetic force equation of the LPMSM is

$$F = \sqrt{\frac{2}{3}} \frac{\pi}{\tau} i_{qs}^e \lambda_m \quad (4)$$

### 3. Planning and Design of Feedback Linearization and Robust Control Mechanisms

The proposed feedback linearization and robust control system for LPMSM is shown in Figure 1. This scheme involves the concept of feedback linearization in the design of a controller based on electromagnetic force, speed and position to correct for errors in tracking control. As shown in Figure 1, the output  $Y$  and input  $R$  can be expressed as the feedback and command values of electromagnetic force, speed and position, respectively. Firstly, the complex and nonlinear status items of linear motors can be converted into a simple linear loop via a feedback linearization control loop. Then, in order to avoid uncertainties in parameters such as temperature or instability of the load is in motion, a strong self-adjuster is needed to increase the stability of the control system. We designed a robust self-tuning controller to increase the stability of the system, so that the error of electromagnetic force command error, speed command error and position command error can be reduced to zero. The advantage is that the entire derivation process is mathematically verified, and the calculations are not complex, providing an alternative approach to motor servo control. The details of system component design are described below.

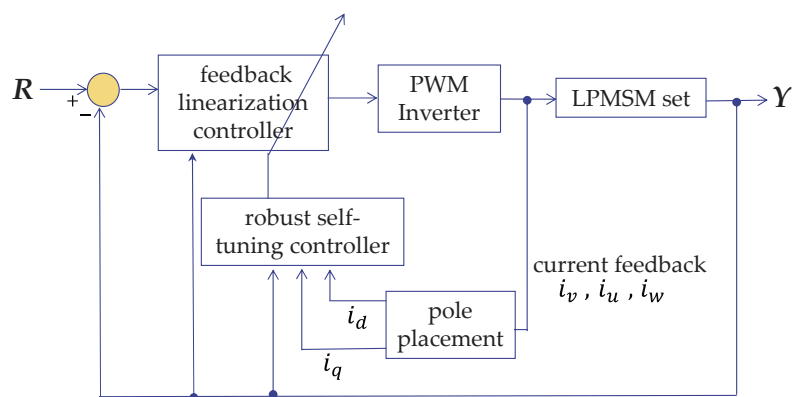


**Figure 1.** Block diagram of the linear permanent magnet synchronous motors (LPMSM) control system.

#### 3.1. Feedback Linearization Controller

Feedback linearization control is based on the use of additional control commands, such that all the dynamic components (including nonlinear components) in a nonlinear system are replaced with linear components. The objective is for the controller to obtain a linear system from a nonlinear one. Conventional linear control theory is easily applied to the processing of linear control problems.

In the following, we give a brief description of the relevant theory. Suppose there is a nonlinear system whose equation of state is written as:

$$\frac{d^n x}{dt^n} = x^{(n)} = f(x) + b(x) u \tag{5}$$

where  $u$  is a scalar input;  $x$  is a scalar output and a state variable equaling  $x = [x \dot{x} \dots x^{(n-1)}]^T$ ;  $f(x)$  and  $b(x)$  are both nonlinear equations of state. As shown in Equation (5), the differential term of  $x$  appears in the equation, but the differential term of input  $u$  does not. Thus, Equation (5) can be written in the standard form below:

$$\frac{d}{dt} \begin{bmatrix} x_1 \\ \dots \\ x_{n-1} \\ x_n \end{bmatrix} = \begin{bmatrix} x_2 \\ \dots \\ x_n \\ f(x) + b(x) u \end{bmatrix} \tag{6}$$

With the following input (assuming  $\frac{1}{b}$  is a nonzero term), a single control command can be designed for feedback linearization.

$$u = \frac{1}{b} \{v - f\} \tag{7}$$

Substituting Equation (5) into Equation (6) gives us

$$x^{(n)} = v \tag{8}$$

Clearly, the nonlinear terms in Equation (5) of the original nonlinear system can be eliminated using Equation (6), resulting in the simple input–output relationship in Equation (8), as shown in Figure 2.

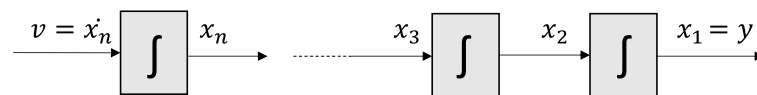


Figure 2. Block diagram after feedback linearization.

Thus, let the control law be written as follows:

$$v = -k_0 x - k_1 \dot{x} - \dots - k_{n-1} x^{(n-1)} \tag{9}$$

where the  $k_1$  value can be used to place all of the roots of polynomial  $P^n + k_{n-1}P^{n-1} + \dots + k_0 = 0$  on the left side of the complex plane and create exponential stability for the dynamics of the differential equation below so that  $x(t) \rightarrow 0$ :

$$x^{(n)} + k_{n-1}x^{(n-1)} + \dots + k_0x = 0 \tag{10}$$

If the output includes a tracking task, and the target output is  $x_d(t)$ , then the control law can be changed to

$$v = x_d^{(n)} - k_0 e - k_1 \dot{e} - \dots - k_{n-1} e^{(n-1)} \tag{11}$$

where  $e(t) = x(t) - x_d(t)$  is the tracking error, and exponential convergence can be achieved.

Note that the condition necessary for our control law to hold true is that the control in Equation (7) must hold true. In areas where  $\frac{1}{b}$  does not exist, the controller will fail. Thus, the characteristics of feedback linearization control theory must also be taken into consideration to prevent them affecting the final response characteristics of the motor system.

### 3.2. Electromagnetic Force Loop Design Based on Feedback Linearization

#### 3.2.1. Tracking Error Analysis in Electromagnetic Force Control

The proposed feedback linearization loop uses electromagnetic force commands for the tracking control of reference commands, so that the electromagnetic force error converges to zero with time. Therefore, we focused on the electromagnetic force,  $\eta_F$ , and based the design of the controller on this error to achieve our tracking objectives.

$$\eta_F = u_F - \sqrt{\frac{2}{3}} \frac{\pi}{\tau} \varphi_F'' i_{qs} \quad (12)$$

where  $u_F$  is the electromagnetic force command.

Differentiation of the electromagnetic force error in Equation (12) results in

$$\dot{\eta}_F = \dot{u}_F - \frac{d}{dt} \left( \sqrt{\frac{2}{3}} \frac{\pi}{\tau} \varphi_F'' i_{qs} \right) \quad (13)$$

$$\dot{\eta}_F = \dot{u}_F + \sqrt{\frac{2}{3}} \frac{\pi^2}{\tau^2} \varphi_F'' \dot{x}_p i_{ds} + \sqrt{\frac{2}{3}} \frac{\pi}{\tau} \varphi_F'' \frac{R_s}{L_s} i_{qs} - \sqrt{\frac{2}{3}} \frac{\pi}{\tau} \varphi_F'' \frac{v_{gs}}{L_s} + \frac{2}{3} \frac{\pi^2}{\tau^2} \varphi_F''^2 \dot{x}_p \frac{1}{L_s} \quad (14)$$

which can be rewritten as

$$\dot{\eta}_F = \Omega_1 + \Omega_2 - \left( \sqrt{\frac{2}{3}} \frac{\pi}{\tau} \varphi_F'' \frac{1}{L_s} v_{qs} \right) \quad (15)$$

Here, we set two variables  $\Omega_1$  and  $\Omega_2$ , defined as

$$\begin{aligned} \Omega_1 &= \dot{u}_F \\ \Omega_2 &= \sqrt{\frac{2}{3}} \frac{\pi^2}{\tau^2} \varphi_F'' \dot{x}_p i_{ds} + \sqrt{\frac{2}{3}} \frac{\pi}{\tau} \varphi_F'' \frac{R_s}{L_s} i_{qs} + \frac{2}{3} \frac{\pi^2}{\tau^2} \varphi_F''^2 \dot{x}_p \frac{1}{L_s} \end{aligned}$$

In Equation (15), if the controller design is

$$\sqrt{\frac{2}{3}} \frac{\pi}{\tau} \varphi_F'' \frac{1}{L_s} v_{qs} = K_P \eta_F + \Omega_1 + \Omega_2 \quad (16)$$

where  $K_P$  is a positive number, then the closed-loop dynamic equation of electromagnetic force error can be expressed as

$$\dot{\eta}_F = -K_P \eta_F \quad (17)$$

The dynamic error equation becomes a simple differential equation. With  $\sqrt{\frac{2}{3}} \frac{\pi}{\tau} \varphi_F'' \frac{1}{L_s} v_{qs}$ , the electromagnetic force error becomes an increasingly stable dynamic system.

Analysis of tracking error in electromagnetic force control eliminates the unknowns from the equation once the only parameter  $K_P$  in Equation (17) is established, thereby rendering the entire system equivalent to a linear system. Conventional control theory can be used to set this parameter. If settling time is the only design condition, then the relationship between settling time  $t_s$  and parameter  $K_P$  with steady state error less than 1% can be written as follows:

$$K_P = \frac{4.6}{t_s} \quad (18)$$

where  $K_P$  is a positive number.

#### 3.2.2. Robust Control Mechanisms for Electromagnetic Force

If the system parameters in a linear feedback controller can be determined with a high degree of precision, then the characteristics of the system will approximate those of the simplified model

in Equation (17). If researchers are unable to obtain precise parameter values, then there will be discrepancies between the actual system and the simplified model, resulting in unexpected (unstable) responses in the system. Thus, we added a robust controller to the linear feedback controller to compensate (Tang et al., 2015).

To correct for error in the feedback controller, the error between the simplified model and the actual system must first be quantified. Here, we make the correction using an increment and revise Equation (16) as follows:

$$\sqrt{\frac{2}{3}} \frac{\pi}{\tau} \varphi_F'' \frac{1}{L_s} (v_{qs} + \Delta v_{qs}) = K_p \eta_F + \Omega_1 + \Omega_2 \tag{19}$$

Thus, we can substitute Equations (13) and (17) into Equation (19) to derive  $\Delta v_{qs}$ :

$$\Delta v_{qs} = -v_{qs} + i_{qe} R_s + \dot{x}_P i_{de} \frac{\pi}{\tau} L_s + \dot{x}_P \sqrt{\frac{2}{3}} \frac{\pi}{\tau} \varphi_F'' + i_{qe} \sqrt{\frac{2}{3}} \frac{\pi}{\tau} \varphi_F'' \tag{20}$$

In Equation (19), we use the increment correction method and add an error correction term  $\Delta v_{qs}$  to the stator voltage command variable in the simplified model. The composition of this correction term is based on disturbances to the linear feedback controller caused by parameter identification errors. The design of the error correction term  $\Delta v_{qs}$  is based on discrete time state. After calculating the robust control mechanism, the  $v_{qs}$  value calculated from the electromagnetic force error input into the system control block serves as the next error correction term to be input into the linear feedback controller.

Figure 3 presents block diagrams showing the design of the robust controller and the feedback linearization controller for electromagnetic force. Experiments and simulations have validated their real-time control performance, as described in Section 4.

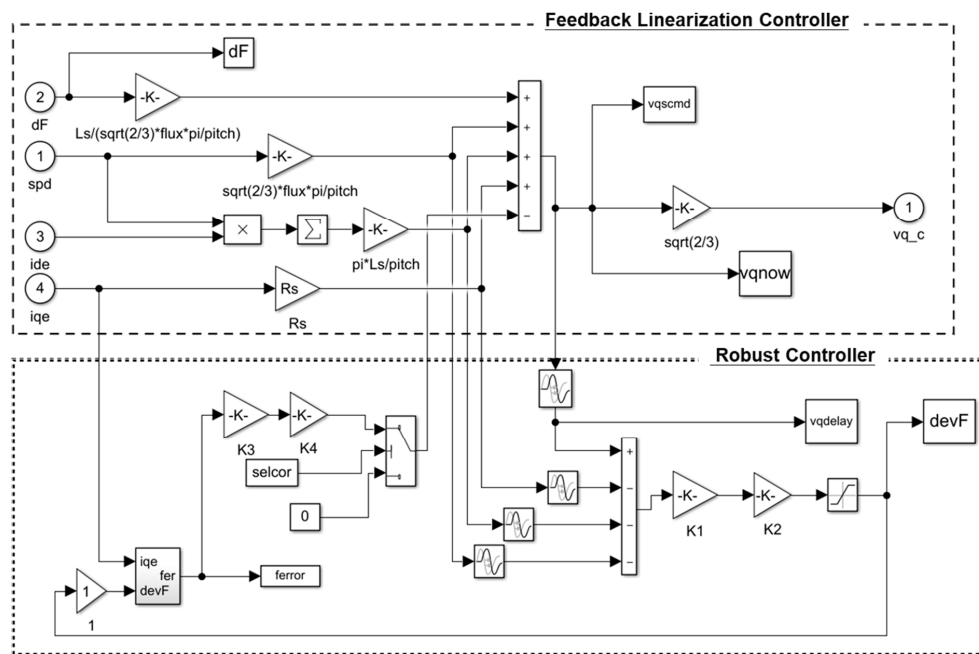


**Figure 3.** Design block diagrams of robust and feedback linearization controller for electromagnetic force control system.

### 3.3. Speed and Position Control Loop Design Based on Feedback Linearization

In this study, we used the electromagnetic force control method derived from feedback linearization theory for the design of the internal loop. In terms of speed and position control, performance standards

for the control performance of high-performance LPMSM-driven systems are rising. This has imposed the two following requirements:

- (1) The steady state error of input and output commands in the system must remain zero.
- (2) The output responses of the control system must be insensitive to changes in LPMSM parameters.

Thus, we also added a robust self-tuner to the position controller to enable automatic self-tuning by the controller based on the input and output signals of the system to make it robust. This mitigates the influence of fluctuations in system parameters, while overcoming the shortcomings of conventional PI controllers, which gives the resulting LPMSM-driven system robust position control performance.

### 3.3.1. Tracking Error in Speed Control

First, the mechanical mathematical model of LPMSMs can be expressed as

$$F = M \frac{d\dot{x}_p}{dt} + \beta \dot{x}_p + F_L \quad (21)$$

where  $M$  is the mass of the mover (kg),  $\beta$  denotes the viscous friction coefficient,  $F_L$  is the load of the LPMSM,  $\dot{x}_p$  indicates the speed of the LPMSM mover (m/s) and  $x_p$  is the position of the primary mover platform.

To obtain the tracking error in position control, we first define the speed error as  $\eta_V$  and design a controller based on this error to achieve our tracking objective.

$$\eta_V = u_V - \dot{x}_p \quad (22)$$

where  $u_V$  is the speed command.

Differentiation of the speed error in Equation (22) results in

$$\dot{\eta}_V = \dot{u}_V - \frac{d\dot{x}_p}{dt} = \dot{u}_V - \frac{F - \beta \dot{x}_p}{M} \quad (23)$$

which can be rewritten as

$$\dot{\eta}_V = \dot{u}_V + \frac{\beta \dot{x}_p}{M} - \frac{F}{M} \quad (24)$$

In Equation (24), if the controller design is written as

$$\frac{F}{M} = \dot{u}_V + \frac{\beta \dot{x}_p}{M} + \left( K_P + \frac{K_i}{s} \right) \eta_V \quad (25)$$

where  $K_P$  and  $K_i$  are positive numbers, then the closed-loop dynamic equation of speed error can be expressed as

$$\dot{\eta}_V = - \left( K_P + \frac{K_i}{s} \right) \eta_V \quad (26)$$

As shown in Equation (26), the dynamic equation for speed error becomes a simple differential equation. With  $\frac{F}{M}$ , the speed error becomes an increasingly stable dynamic system.

### 3.3.2. Tracking Error in Position Control

In the position control loop, the  $\frac{K_i}{s} \eta_V$  term in Equation (25) can be directly measured by the system and replaced with  $K_i \eta_X$ . The result can then be rewritten as follows:

$$\frac{F}{M} = \dot{u}_V + \frac{\beta \dot{x}_p}{M} + K_P \eta_V + K_i \eta_X \quad (27)$$

where  $K_p$  and  $K_i$  are positive numbers, and  $\eta_X$  is the position error. The closed-loop dynamic equation of speed error can then be expressed as

$$\dot{\eta}_V = -K_p \eta_V - K_i \eta_X \quad (28)$$

### 3.3.3. Pole Placement Method

The mechanical equation in Equation (21) shows that if the load of the LPMSM is zero ( $F_L = 0$ ), then a simple second-order system can be used to place the two poles in the position control loop. Furthermore, a suitable settling time can be set for the position controller based on the response speed of the electromagnetic force controller. Suppose that the settling time of the electromagnetic force controller is 0.01 s, then we set the settling time of the position controller between 0.2 and 0.4 s to avoid system instability. For the sake of convenience, we adopted the conventional linear control theory to design the two poles of the second-order system and set them as a pair of conjugate complex poles, as shown in Figure 4.

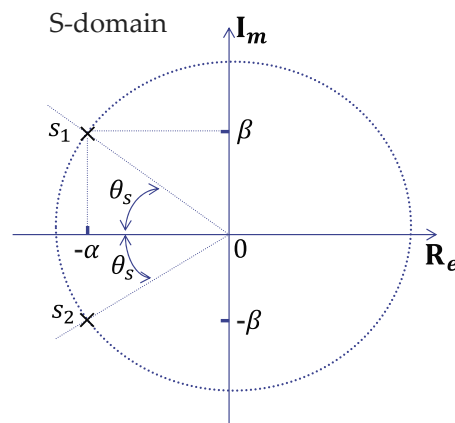


Figure 4. Poles placed on the s-plane.

The positions of the two poles are expressed as

$$s_1, s_2 = \alpha \pm j\beta = \alpha(1 \pm j \tan \theta_s) \quad (29)$$

where  $\alpha$  is associated with the settling time of the system's transient responses; angle  $\theta_s$  is associated with system oscillations and can be set between  $30^\circ$  and  $45^\circ$  based on experience. According to Equations (28) and (29), it can be rewritten as

$$[s - \alpha(1 + j \tan \theta_s)] [s - \alpha(1 - j \tan \theta_s)] = s^2 + K_p s + K_i \quad (30)$$

By expanding Equation (30), we obtain the following formulas:

$$\begin{aligned} K_p &= -2\alpha \\ K_i &= \alpha^2(1 + \tan^2 \theta_s) \end{aligned} \quad (31)$$

If settling time is the only design condition, then the relationship among settling time  $t_s$  and parameters  $\alpha$ ,  $K_p$  and  $K_i$  with  $\theta_s = 30^\circ$  and steady state error less than 1% can be written as

$$\alpha = -\frac{4.6}{t_s}, K_p = \frac{9.2}{t_s}, K_i = \frac{28.2133}{t_s^2} \quad (32)$$

where  $K_p$  and  $K_i$  are positive numbers.

The nonlinear equation in Equation (23) has already been replaced with linear Equations (26) and (28) using the linear feedback control tracking error command; therefore, parameters  $K_p$  and  $K_i$  have nothing to do with the operating points of the system itself. This controlled system can be regarded as a system with global stability. At the same time, all the variables in the control tracking error commands in Equations (23) and (26) can be measured using a PC-based control architecture system, thereby expanding the applicability of the controller.

### 3.3.4. Robust Control Mechanisms for Position

Although the two poles established using the pole placement method can be proven based on conventional linear control theory, they do not meet the two requirements established in academia and industry with regard to the control performance of LPMSM-driven systems. Thus, we added a robust control mechanism to the position control loop to produce a controller with good speed performance. Correcting for errors in state feedback from the controller requires that we first quantify the error and then make the correction using an incremental approach. Equations (25) and (27) can be revised as follows:

$$\frac{F + \Delta F}{M} = \dot{u}_V + \frac{\beta \dot{x}_p}{M} + \left( K_P + \frac{K_i}{s} \right) \eta_V \tag{33}$$

$$\frac{F + \Delta F}{M} = \dot{u}_V + \frac{\beta \dot{x}_p}{M} + K_P \eta_V + K_i \eta_X \tag{34}$$

Thus, substituting Equations (23), (26) and (28) into Equations (33) and (34) gives us the following:

$$\Delta F = \left[ \frac{d\dot{x}_p}{dt} - \left( \frac{F - \beta \dot{x}_p}{M} \right) \right] \times M \tag{35}$$

In Equation (23), we use the increment correction method and add an error correction term  $\Delta F$  to the electromagnetic force command variable in the position controller. The composition of this correction term is determined by disturbance associated with the linear feedback controller caused by parameter identification errors. The design of the error correction term  $\Delta F$  is based on a discrete time state. The  $F$  value input into the system control block (calculated from the speed and position error) serves as the next error correction term input into the linear feedback controller.

Figures 5 and 6 display block diagrams showing the design of the robust controller and the feedback linearization controller for speed and position. Experiments and simulations verify their real-time control performance in the next section.

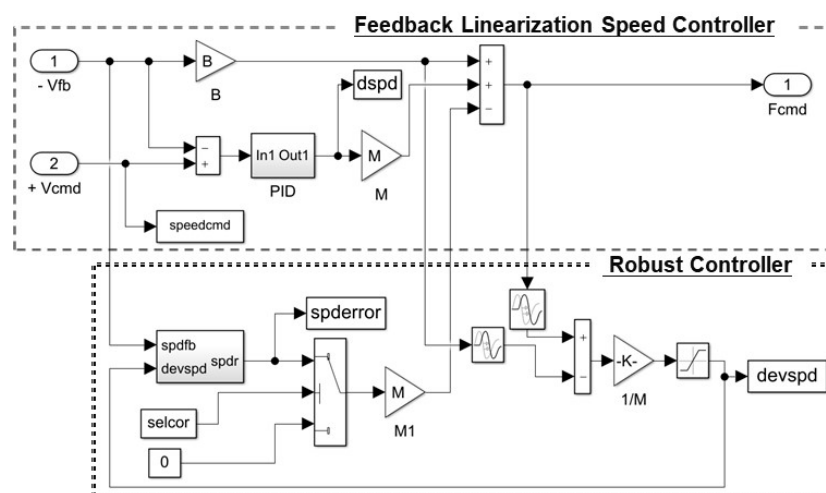


Figure 5. Design block diagrams of robust controller and feedback linearization speed controller.

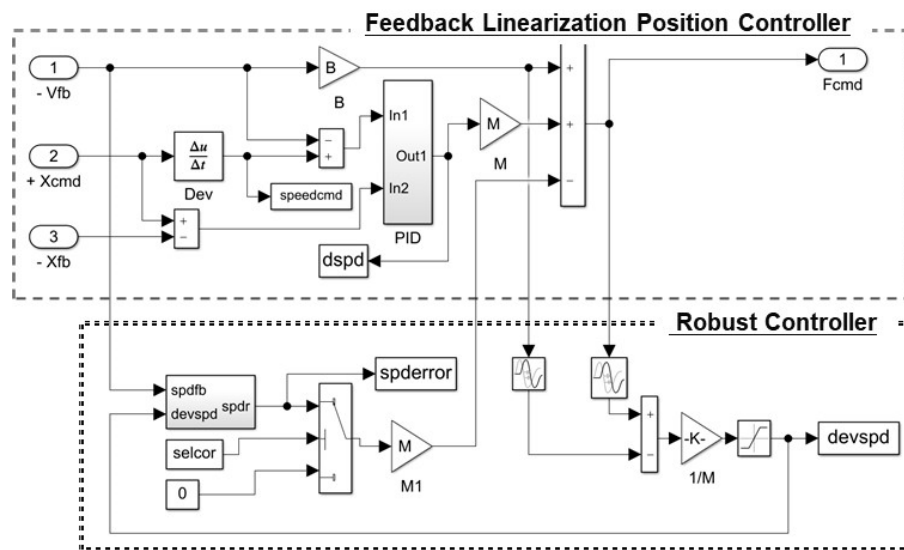


Figure 6. Design block diagrams of robust controller and feedback linearization position controller.

## 4. Experiment System and Realization

### 4.1. Experiment System

This section outlines the hardware and methods required to realize an LPMSM with feedback linearization. We adopted a PC-based control architecture and 83W 220V three-phase two-pole LPMSM ( $\Delta$  connection). The LPMSM experiment system includes the LPMSM itself, an incremental encoder, an amplifier (power stage), a motor control driver interface card and a control platform (personal computer). The motor control driver interface card was connected to an ISA bus, the input/output ports and IRQ which were used for data and signal communication. Figure 7 displays the PC-based LPMSM experiment system. The LPMSM parameters used in the simulation and experiment are listed in the Appendix A.

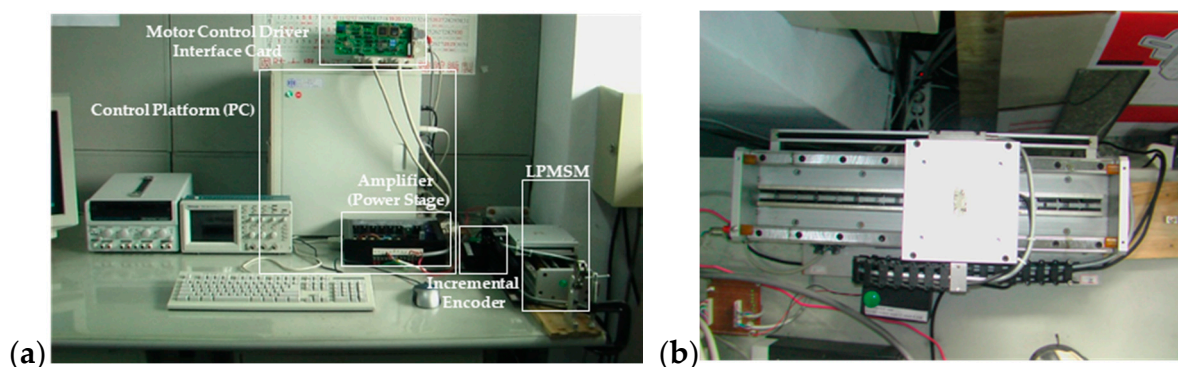


Figure 7. (a) PC-based LPMSM experiment system. (b) The top view of LPMSM.

### 4.2. Results of Simulations and Experiments on Feedback Linearization and Robust Control Mechanisms

We simulated the proposed electromagnetic force, speed and position control mechanisms for LPMSMs using MATLAB/SIMULINK and a PC-based motor control system. The parameters of the LPMSM used in the experiment were identical to those of the motor in the computer simulation. To avoid instabilities caused by errors in the response speeds during the experiment, we employed conventional linear control theory and robust controllers for electromagnetic force and position control in the feedback linearization control architecture to enable self-error correction.

The proposed robust controllers input electromagnetic force, speed and position command errors into the feedback linear controllers, which calculate the voltage vectors that are required. Once the linear motor system is working, feedback current measurements are sent back to the feedback controller via the robust self-tuning mechanism to execute operation control. In the following, we discuss the simulations and experiments based on the control law derived from feedback linearization and robust control.

#### 4.2.1. Electromagnetic Force Control Loop Experiment Top View

- Accuracy test of feedback linearization controller

The purpose of this experiment was to verify the accuracy of the feedback linearization controller and its effects on the system. We used sinusoidal and trapezoidal waves as electromagnetic force commands (period: 2 s, amplitude: 20 N). Using accurate control system parameters (electrical and mechanical), we compared the responses of the system in simulations and experiments, as shown in Figures 8 and 9. The dashed lines (—) represent the input electromagnetic force command curves, and the bold lines (—) represent the electromagnetic force response curves: (a) displays the responses of the system, whereas (b) presents the responses of the system in experiments. Our simulation and experiment results both show that when using accurate motor parameters, the system can achieve the expected control results.

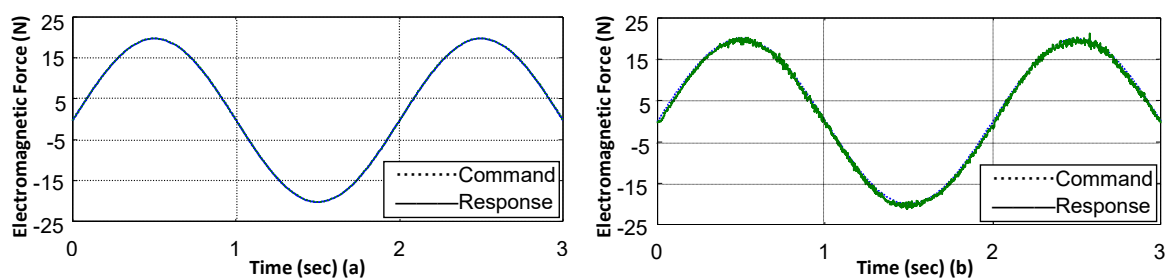


**Figure 8.** Feedback linearization control experiment—simulated (a) and measured (b) responses from 3 (sine wave) commands.

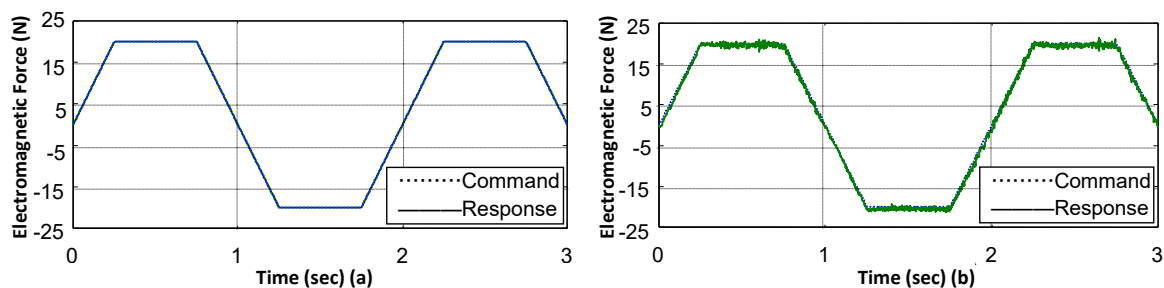


**Figure 9.** Feedback linearization control experiment—simulated (a) and measured (b) responses from electromagnetic force (trapezoidal wave) commands.

- Robust control test under parameter disturbance

Our objective in this test was to verify that the robust controller is capable of self-tuning (to achieve good control performance) in the event of disturbances in the parameters of the controlled system. Trapezoidal waves were used as electromagnetic force commands (period: 2 s, amplitude: 20 N), and the stator flux was set at 1.5 times the original setting, as shown in Figure 10. Among the system parameters, the stator flux and resistivity were both set at 1.5 times the original settings, as shown in Figure 11. The two Figures, respectively, compare the actual responses in the system when only

a feedback linearization controller was used and when an additional robust controller was used. The dashed lines (—) represent the input electromagnetic force command curves, and the bold lines (—) represent the electromagnetic force response curves: (a) displays the responses of the system in the experiment when only a feedback linearization controller was used; (b) displays the responses of the system in the experiment when an additional robust controller was used. These experiment results show that even in the event of disturbances in the motor parameters, the self-tuning function of the additional robust controller is able to maintain good system performance.

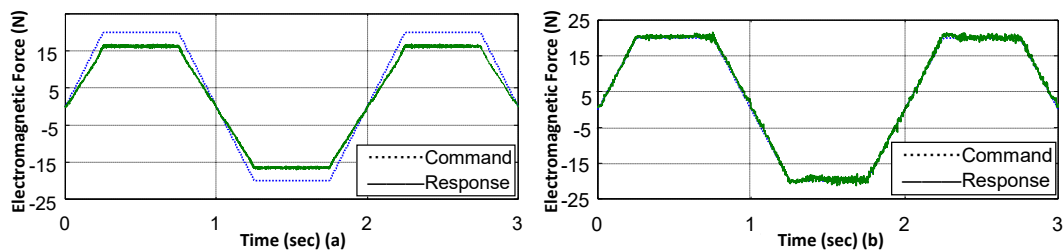


**Figure 10.** Measured responses from electromagnetic force (trapezoidal wave) commands with stator flux set to 1.5 times the original setting: (a) feedback linearization controller only; (b) robust control mechanism added.

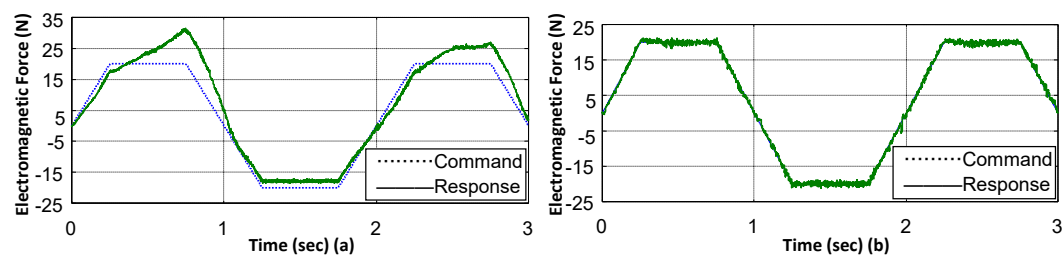


**Figure 11.** Measured responses from electromagnetic force (trapezoidal wave) commands with stator flux and resistivity changed to 1.5 times the original settings: (a) feedback linearization controller only; (b) robust control mechanism added.

#### 4.2.2. Position Control Loop Experiment

- Accuracy test of feedback linearization controller

Our objective in this experiment was to verify the accuracy of feedback linearization controller and its effects on the system. Sine waves and trapezoidal waves were used as position input commands (period: 2 s, amplitude: 0.03 m). Using accurate control system parameters (electrical and mechanical), we compared the responses of the system in simulations and experiments, as shown in Figures 12 and 13. The dashed lines (—) represent the input position command curves, and the bold lines (—) represent the position response curves: (a) displays the response of the system in simulations; (b) displays the responses of the system in experiments. These simulation and experiment results both show that when using accurate motor parameters, the system can achieve the expected control results.

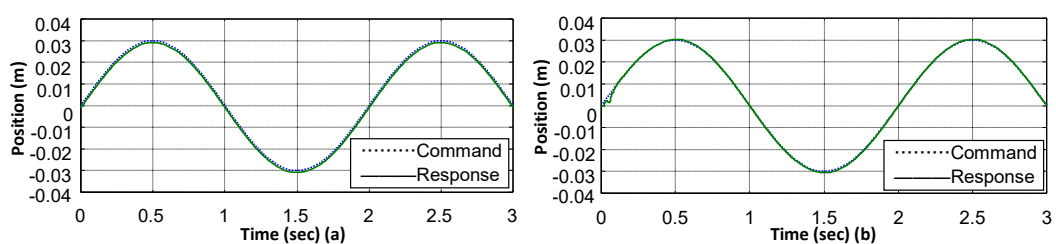


**Figure 12.** Feedback linearization control experiment—(a) simulated and (b) measured responses from position (sine wave) commands.

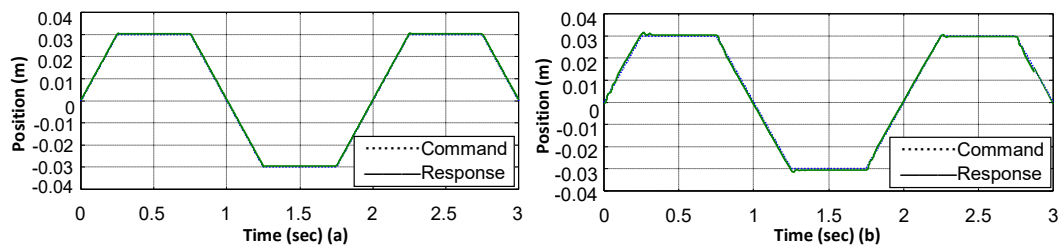


**Figure 13.** Feedback linearization control experiment—(a) simulated and (b) measured responses from position (trapezoidal wave) commands.

- Robust control tested under parameter disturbance

Our objective in this test was to verify that the controller is capable of self-tuning in the event of disturbances in the parameters of the controlled system. Trapezoidal waves were used as position input commands (period: 2 s, amplitude: 0.03 m), and among the parameters of the controlled system, the stator flux was set at 1.5 times the original setting, as shown in Figure 14. Among the system parameters, the stator flux and resistivity were both set at 1.5 times the original settings, as shown in Figure 15. These two Figures compare the actual responses of the system when using only a feedback linearization controller and when using an additional robust controller, respectively. The dashed lines (—) represent the input position command curves, and the bold lines (—) represent the position response curves: (a) displays the responses of the system in the experiment when only a feedback linearization controller was used; (b) displays the responses of the system in the experiment when an additional robust controller was used. These experiment results show that in the event of disturbances in the motor parameters, the self-tuning function of the additional robust controller can achieve good system performance.

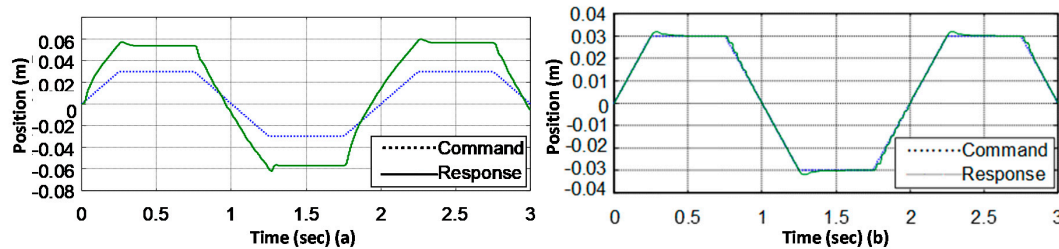


**Figure 14.** Measured responses from position (trapezoidal wave) commands with stator flux changed to 1.5 times the original setting: (a) feedback linearization controller only; (b) robust control mechanism added.

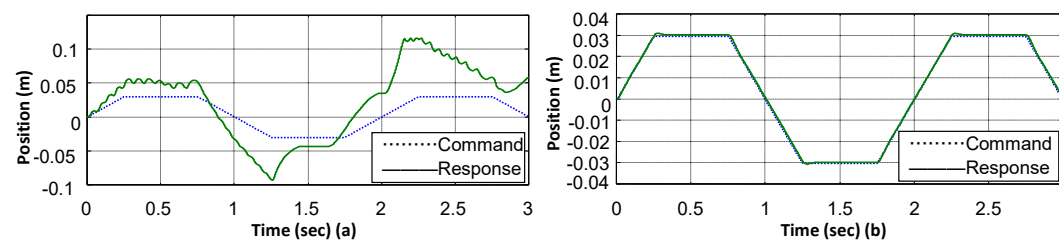


**Figure 15.** Measured responses from position (trapezoidal wave) commands with stator flux and resistivity changed to 1.5 times the original settings: (a) feedback linearization controller only; (b) robust control mechanism added.

- Settling time test

Our objective in this experiment was to ensure that the proposed robust controller adapts to the application environment and set the settling time of the system and the control performance of the

anti-disturbance of motor parameter disturbance. Trapezoidal waves were used as input commands (period: 2 s, amplitude: 0.03 m), as shown in Figures 16 and 17. In (a), the electrical and mechanical parameters of the controlled system were accurate, whereas in (b), the stator flux and resistivity were both set at 1.5 times the original settings. The dashed lines (—) represent the input position command curves; (—□—□—), (—○—○—) and (—△—△—), show the speed and position response curves with system settling times of 0.2, 0.3, and 0.4 s, respectively. Using Equation (32), we obtain the following results:

$$t_s = 0.2, K_p = 46, K_d = 705.3333$$

$$t_s = 0.3, K_p = 30.6667, K_d = 313.4815$$

$$Zt_s = 0.4, K_p = 23, K_d = 176.3333$$

These experiment results demonstrate that the proposed robust controller is able to adjust the settling time based on the application environment to meet the operating points required by the various controllers. For instance, it is able to set the optimal efficiency point in system operations for optimal control.

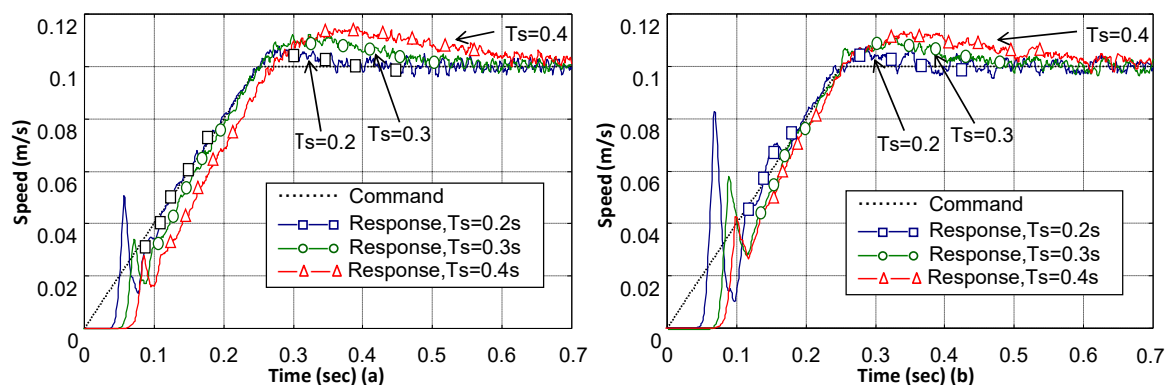


**Figure 16.** Settling time tests of feedback linearization controller with robust control—measured responses from speed (trapezoidal wave): (a) original parameter settings; (b) stator flux changed to 1.5 times the original settings.

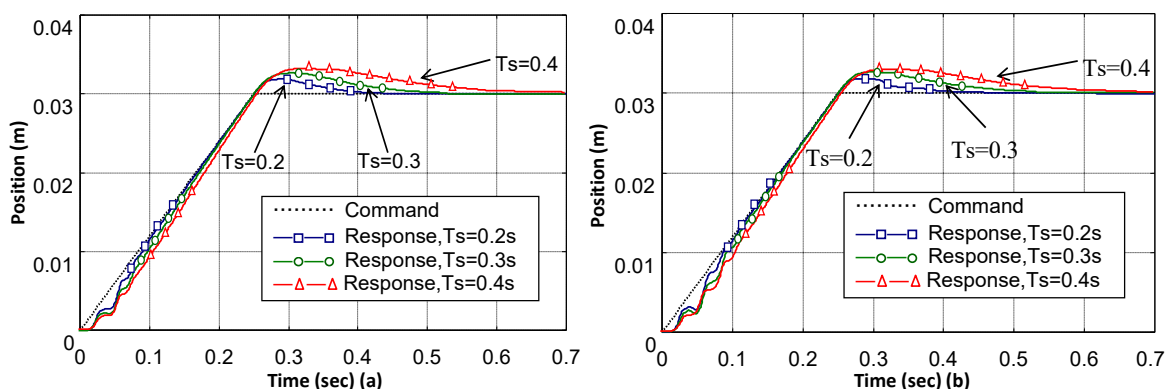


**Figure 17.** Settling time tests of feedback linearization controller with robust control—measured responses from position (trapezoidal wave): (a) original parameter settings; (b) stator flux changed to 1.5 times the original settings.

## 5. Results and Discussion

Our experiment results show that our robust control law designed using feedback linearization produces good electromagnetic force and position responses, regardless of whether it is transient or steady state. In terms of response speed, the proposed control method uses parameters  $K_p$  and  $K_i$  to change the response speeds of electromagnetic force and position to achieve a suitable settling

time to meet the operating points required by the various controllers. The inclusion of the robust controller enables the system to remain within a stable range by removing interference from factors that do not remain steady under all conditions. Table 1 displays the root mean square error (RMSE) between measure and command value of electromagnetic force, speed and position. As shown in the table, the addition of the robust controller to the feedback linearization control system resulted in lower smaller root mean square error values than those in a conventional feedback linearization control. This demonstrates the accuracy and effectiveness of the robust control strategy with feedback linearization developed in this study.

**Table 1.** Root mean square error (RMSE) between measure and command value.

Experiment		Controller	
		Conventional Feedback Linearization Controller	Robust Control Mechanism Added
Command of Electromagnetic thrust (20 N)	Original parameter settings	1.7183	0.3929
	stator flux and resistivity changed to 1.5 times the original settings	2.6719	0.5095
Command of speed (0.1 m/s)	Original parameter settings	0.0089	0.0056
	stator flux and resistivity changed to 1.5 times the original settings	0.022	0.0063
Command of position (0.03 m)	Original parameter settings	0.0033	0.000393
	stator flux and resistivity changed to 1.5 times the original settings	0.0161	0.00048394

Root mean square formula :  $\left[ \frac{1}{N} \sum_{i=1}^N (\text{Measure value} - \text{Command value})^2 \right]^{\frac{1}{2}}, N = 1000$

Table 2 shows the root mean square error (RMSE) between the simulation and measure value of electromagnetic force, speed and position. As shown in the table, the inclusion of the robust controller in the feedback linearization control system resulted in much lower root mean square error values than those obtained using a conventional feedback linearization control system.

**Table 2.** Root mean square error (RMSE) between simulation and measure value.

Experiment		Controller	
		Conventional Feedback Linearization Controller	Robust Control Mechanism Added
Command of Electromagnetic thrust (20 N)	Original parameter settings	1.6891	0.3833
	stator flux and resistivity changed to 1.5 times the original settings	12.8633	0.4954
Command of speed (0.1 m/s)	Original parameter settings	0.0089	0.0027
	stator flux and resistivity changed to 1.5 times the original settings	0.0262	0.0062
Command of position (0.03 m)	Original parameter settings	0.0033	0.000359
	stator flux and resistivity changed to 1.5 times the original settings	0.0179	0.00048224

Root mean square formula :  $\left[ \frac{1}{N} \sum_{i=1}^N (\text{Measure value} - \text{Command value})^2 \right]^{\frac{1}{2}}, N = 1000$

Our simulation and experiment results indicate that the proposed robust control method based on feedback linearization produces better responses than conventional feedback linearization control when fluctuating factors produce disturbances in the system parameters. Furthermore, the expected settling time values can be adjusted according to the application environment to maintain the operational performance. The robustness of the proposed control method makes it suitable for a wider range of operations. The proposed feedback linearization controller with robust performance offers the following advantages:

- (1) It is applicable to electromagnetic force as well as position control loop systems in motor control.
- (2) It does not require complex mathematical formulas—i.e., the error correction term is added using a simple increment correction method.
- (3) It can establish an appropriate system settling time based on the application environment.

## 6. Conclusions

In this study, we designed a feedback linearization control strategy for LPMSMs with robust control mechanism to overcome the shortcomings of conventional feedback linearization schemes. The management of nonlinear controlled systems to achieve system linearity is based on feedback linearization control theory. We also designed a robust controller to mitigate the impact of system parameter disturbances on system performance. This novel robust feedback controller is applicable to electromagnetic force, speed and position control loops in linear motors. It can also be used to correct for errors caused by unpredictable fluctuations in real-time and establish an appropriate settling time based on the application environment. In other words, a simple and robust controller design that does not require complex calculations is needed for feedback linearization when the ultimate objective is to enhance the precision of the motor speed and position in a wide range of industrial applications. Owing to the validation of the optimization and effectiveness of the proposed scheme, a feedback linearization based robust control simulation is constructed as an application paradigm. The integration test results show that the proposed development scheme can certainly comply with the design objectives.

**Author Contributions:** Y.-T.C. performed the experiments; P.-N.C. wrote the manuscript; C.-S.Y. and P.-N.C. provided the concept and experimental design of the study and reviewed the paper prior to submission. All authors discussed the results, analyzed the data and commented on the manuscript. All authors have read and agreed to the published version of the manuscript.

**Funding:** This research received no external funding.

**Acknowledgments:** The current study was supported by grants from the Ministry of National Defense—Medical Affairs Bureau (MAB-109-083).

**Conflicts of Interest:** The authors declare no conflict of interest.

## Appendix A

LPMSM Mechanical Parameters:  $M = 3.0513 \text{ kg}$ ,  $\beta = 46.0384 \frac{\text{N}}{\text{m.s}}$ , pole pitch = 0.06096 m.  
 Electrical Parameters:  $R_s = \frac{17.7}{3} \Omega$ ,  $L_s = L_d = L_q = \frac{0.0063}{3} \text{H}$ ,  $\varphi = 0.4849 \text{ WB}$ .

## References

1. Gieras, J.F.; Piech, Z.J.; Tomczuk, B.Z. *Linear Synchronous Motors: Transportation and Automation Systems*, 2nd ed.; CRC Press: Boca Raton, FL, USA; Taylor & Francis: Florida, FL, USA, 2000.
2. Jawad, F.; Mehdi, M.; Ghazanfar, S. A Novel Robust Design for LPMSM with Minimum Motor Current THD Based on Improved Space Vector Modulation Technique. In Proceedings of the IEEE Electrical Machines & Power Electronics (ACEMP), Side, Turkey, 2–4 September 2015.
3. Huikuri, M.T.; Jansen, J.; Lomonova, E.A.; Pyrhönen, J.J. Adaptive Feedforward Control of an Industrial H-Drive Positioning with Permanent Magnet Linear Motors. *Int. Rev. Model. Simul. (IREMOS)* **2015**, *8*, 399. [[CrossRef](#)]

4. Ghafari-Kashani, A.; Faiz, J.; Yazdanpanah, M. Integration of non-linear  $H_{\infty}$  and sliding mode control techniques for motion control of a permanent magnet synchronous motor. *IET Electr. Power Appl.* **2010**, *4*, 267. [[CrossRef](#)]
5. Choi, H.H.; Jung, J.-W.; Kim, R.-Y. Fuzzy adaptive speed control of a permanent magnet synchronous motor. *Int. J. Electron.* **2012**, *99*, 657–672. [[CrossRef](#)]
6. Ananthamoorthy, N.P.; Baskaran, K. Modelling, Simulation and Analysis of Fuzzy Logic Controllers for Permanent Magnet Synchronous Motor Drive. *Int. Rev. Model. Simul.* **2013**, *6*, 75–82.
7. Pei, P.; Pei, Z.; Tang, Z.; Gu, H. Position Tracking Control of PMSM Based on Fuzzy PID-Variable Structure Adaptive Control. *Math. Probl. Eng.* **2018**, *2018*, 1–15. [[CrossRef](#)]
8. Rubio, J.D.J. Robust feedback linearization for nonlinear processes control. *ISA Trans.* **2018**, *74*, 155–164. [[CrossRef](#)] [[PubMed](#)]
9. Oh, S.-Y.; Choi, H.-L. On Robust Approximate Feedback Linearization: Control with Two Gain-scaling Factors. *Int. J. Control. Autom. Syst.* **2020**, *18*, 1–8. [[CrossRef](#)]
10. Song, X.J. Design and Simulation of PMSM Feedback Linearization Control System. *TELKOMNIKA* **2013**, *11*, 1245–1250.
11. Moradi, O.; Pahlavani, M.R.A.; Soltani, I. High Performance Feedback Linearization Control of Induction Motor. *Int. J. Electron. Commun. Comput. Eng.* **2015**, *5*, 2278–4209.
12. Lin, C.-H. Precision Motion Control of a Linear Permanent Magnet Synchronous Machine Based on Linear Optical-Ruler Sensor and Hall Sensor. *Sensors* **2018**, *18*, 3345. [[CrossRef](#)] [[PubMed](#)]
13. Westenbroek, T.; Fridovich-Keil, D.; Mazumdar, E. Feedback linearization for Unknown Systems via Reinforcement Learning. In Proceedings of the 2020 IEEE International Conference on Robotics and Automation (ICRA), Paris, France, 1–8 August 2020.
14. Lin, C.-H. Linear permanent magnet synchronous motor drive system using AAENNB Control system with error compensation controller and CPSO. *Electr. Eng.* **2020**, *102*, 1311–1325. [[CrossRef](#)]
15. Jiménez, A.; Al-Hadithi, B.; Pérez-Oria, J.; Alonso, L. Optimal Control Using Feedback Linearization for a Generalized T-S Model. In *Artificial Intelligence Applications and Innovations. AIAI 2014: IFIP Advances in Information and Communication Technology, Rhodes, Greece, 19–21 September 2014*; Springer: Berlin/Heidelberg, Germany, 2014; pp. 466–475.
16. Su, W.-T.; Liaw, C.-M. Adaptive positioning control for a LPMSM drive based on adapted inverse model and robust disturbance observer. *IEEE Trans. Power Electron.* **2006**, *21*, 505–517.
17. Vittek, J.; Vavrůš, V.; Minářech, P.; Faber, J. Forced Dynamics Position Control of the Drive with Linear PMSM and Flexible Coupling. In Proceedings of the 2010 IEEE Region 8 International Conference on Computational Technologies in Electrical and Electronics Engineering (SIBIRCON), Irkutsk Listvyanka, Russia, 11–15 July 2010; pp. 806–811.
18. Tang, C.S.; Liu, H.W.; Dai, Y.H. Robust Optimal Control of Chaos in Permanent Magnet Synchronous Motor with Unknown Parameters. *J. Electr. Syst.* **2015**, *11*, 376–383.
19. Ibtissem, B.; Souad, C.; Abdesselam, M. High Performance Backstepping Control of Induction Motor with Adaptive Sliding Mode Observer. *Arch. Control Sci.* **2011**, *21*, 331–344.
20. Asseu, O.; Ori, T.R.; Ali, K.E.; Yeo, Z.; Ouattara, S.; Lin-Shi, X. Nonlinear Feedback Linearization and Observation Algorithm for Control of a Permanent Magnet Synchronous Machine. *Asian J. Appl. Sci.* **2011**, *4*, 202–210.
21. Song, X.; Xu, D.; Yang, W.; Xia, Y.; Jiang, B. Improved Model-Free Adaptive Sliding-Mode-Constrained Control for Linear Induction Motor Considering End Effects. *Math. Probl. Eng.* **2018**, *2018*, 1–9. [[CrossRef](#)]
22. Wang, S.; Shi, S.S.; Chen, C. Research on Grey Compensation-Prediction PID Controller for PMSM Servo System. In Proceedings of the IEEE Control and Decision Conference (CCDC), Xuzhou, China, 26–28 May 2010.

